ARTICLE

Improvement of Transparent Conducting Nanotube Films by Addition of Small Quantities of Graphene

Paul J. King, Umar Khan, Mustafa Lotya, Sukanta De, and Jonathan N. Coleman*

School of Physics and CRANN, Trinity College Dublin, D2, Ireland

ABSTRACT We demonstrate a water-based method to prepare transparent, conducting graphene/single-walled nanotube hybrid films. While the transmittance decreases slightly with increasing graphene content, the DC conductivity, σ_{DC}, and sheet resistance scale non-monotonically with film composition. We observe an optimum composition of ~3 wt % graphene, which results in a peak in the DC conductivity. We have calculated the figure of merit, the DC to optical conductivity ratio, σ_{DC}/σ_{Op}, which also shows a peak at this composition. We find that this effect is only present for small graphene flakes. In addition, acid treatment increases both the σ_{DC} and σ_{DC}/σ_{Op} by ×2.5. Interestingly, acid treatment is more effective for films close to the optimum composition. This has the effect of sharpening the peaks in both σ_{DC} and σ_{DC}/σ_{Op}. For acid-treated films, addition of 3 wt % graphene results in a 40% increase in σ_{DC}/σ_{Op} compared to the nanotube-only film, from 12.5 to 18. Optimized, acid-treated films display transmittance of 80% coupled with a sheet resistance of 100 Ω/□.

KEYWORDS: graphene · nanotube · hybrid · transparent conductor · resistance · transmittance

The market for high-quality displays is expected to both expand and diversify in coming years. In the near future, such displays will become much more common as highly portable, lightweight computer equipment becomes more widespread. In addition, future displays are expected to be flexible as technology such as e-paper is fully developed. Currently, most displays rely on transparent electrodes which both supply current and allow light to exit.[1] The most common transparent electrode material is indium tin oxide (ITO). However, this material is becoming more expensive as supplies of indium run low. In addition, due to its brittle nature,[2,3] ITO is completely unsuited to flexible devices (although it may play a role in conformable electronics). Finally, the relatively high temperatures associated with the deposition of high-quality ITO rule out its use in conjunction with any plastic substrates.[4] For these reasons, the search is on for new materials to replace ITO. Potential transparent electrode materials must be formable into films at low temperatures, preferably by solution phase processing such as spraying or roll-to-roll coating. These films must have sheet resistance of $R_s < 100\ \Omega/\square$, coupled with visible transmittance of $T > 90\%$.[5] The sheet resistance must be stable under repeated flexing, and the films must be chemically inert and well adhered to the substrate. This set of requirements has meant the group of suitable candidate materials is small.

In order to compare results for different types of candidate materials, it is important to calculate a figure of merit for the transparent conductor under investigation. While a number of figures of merit have been postulated,[1,6,7] probably the best is the ratio of DC to optical conductivity, σ_{DC}/σ_{Op}.[8] The DC conductivity describes charge transport due to constant applied fields, while σ_{Op} controls the motion of electrons in response to optical fields. The optical conductivity is effectively a measure of the imaginary part of the permittivity of the material and hence describes optical absorption through the relationship between the imaginary permittivity and the imaginary part of the refractive index. (We note that σ_{Op} is related to the absorption coefficient, α, by $\sigma_{Op} \approx 2\alpha/Z_0$, where Z_0 is the impedance of free space and is equal to 377 Ω.)[9] The conductivity ratio can be calculated directly from transmittance and sheet resistance data:

$$T = \left(1 + \frac{Z_0}{2R_s}\frac{\sigma_{Op}}{\sigma_{DC}}\right)^{-2} \quad (1)$$

Calculation of σ_{DC}/σ_{Op} does not rely on thickness measurements and represents a simple way of comparing different samples.[10] Note that larger values of σ_{DC}/σ_{Op} give high T, coupled with low R_s. The requirement stated above that $R_s < 100\ \Omega/\square$,

*Address correspondence to colemaj@tcd.ie.

Received for review March 16, 2010 and accepted June 21, 2010.

Published online July 1, 2010.
10.1021/nn100542z

while $T > 90\%$, is equivalent to stating that $\sigma_{DC}/\sigma_{Op} > 35$.

Probably the most promising materials are networks of one- and two-dimensional nanostructures, such as carbon nanotubes or graphene flakes. The reason for this is that thin films formed from these materials tend to be electrically stable under flexing.[11−14] Because the elements of the network are weakly bonded by van der Waals interactions, interconductor (*e.g.*, nanotube−nanotube) junctions can move to relax externally applied stress. However, the electrical transport through such junctions is by tunneling, which is unaffected by such motion. The most commonly studied nanomaterials are metallic nanowires,[11,15−17] single-walled carbon nanotubes (SWNTs),[8,14,18,19] and graphene.[5,12,20,21] Networks of silver nanowires display significant potential. Such networks have been reported to display $\sigma_{DC}/\sigma_{Op} \sim 450$.[11] However, such materials may suffer from stability and adhesion issues. Graphene also displays problems, primarily its due to its high optical absorption.[5,22] The best graphene networks demonstrated have had $\sigma_{DC}/\sigma_{Op} \sim 2$.[5] Nanotube films are probably the most intensely studied material, displaying performance[23] close to that required for industry with reports of σ_{DC}/σ_{Op} between 25 and 35.[18,23] However, while many papers have been published, only marginal improvements have been reported for nanotube films over the past few years. The state of the art[18] for nanotube films has remained virtually unchanged over the last 3 years and stands at $R_s = 100\ \Omega/\square$ for $T \sim 85\%$ (this works out to be equivalent to $\sigma_{DC}/\sigma_{Op} = 25$;[18] while $\sigma_{DC}/\sigma_{Op} = 35$ has been reported, this was for films with lower transmittance, $T \sim 70\%$[23]). Effectively, the conductivity of nanotube networks has not improved over this period, remaining close to 5×10^5 S/m (after post-treatment).[18,19,23] Further improvements are required to challenge indium tin oxide as a viable material for transparent conductors. We believe that this will require a significant shift away from the current strategies of improving film formation and post-treatment techniques.[9,14]

Recently, it was reported that hydrazine-reduced, SWNT/graphene oxide hybrid films displayed improved sheet resistance and transmittance relative to either nanotube-only or graphene-oxide-only films.[24] This result is important as it shows that nanotube films can be improved upon. However, in an industrial setting, the requirement for hydrazine reduction will be a barrier to the uptake of this technology if a cheaper, easier alternative is available. In fact, reduction, either thermally or by chemical treatment, is unnecessary if graphene is used rather than graphene oxide. Recent advances have made the liquid phase processing of graphene possible, allowing the production of graphene/SWNT hybrids.[25−29]

In this work, we demonstrate such a method to prepare graphene/nanotube hybrid films. We build on our previous work which demonstrated that graphene can be exfoliated nondestructively using certain solvents[25,26] or surfactants.[12,27] We show that individual surfactant-stabilized nanotube and graphene suspensions can be blended to prepare hybrid suspensions which can be cast into hybrid films. These hybrid films display an optimum composition of 3 wt % graphene for which the sheet resistance had decreased by ~20% compared to the nanotube-only film. Acid treatment results in a significant decrease in sheet resistance for all films. However, the decrease is proportionally greater for the 3 wt % graphene films compared to the nanotube-only films. The acid-treated, 3 wt % graphene film displayed a sheet resistance that was 32% lower than the nanotube-only film. Production of a range of acid-treated films, all with 3 wt % graphene but different thicknesses, showed that hybrid films with excellent optical and electrical properties could be obtained. For example, a 35 nm thick film displayed $T = 80\%$ and $R_s = 100\ \Omega/\square$.

RESULTS AND DISCUSSION

Flake Size Dependence. Aqueous dispersions of carbon nanotubes and graphene were prepared separately by sonication (see Methods for more detail) using the surfactant, sodium cholate, as a stabilizer, as described previously.[12,27] It is straightforward to prepare thin films of liquid-dispersed nanomaterials by vacuum filtration.[11−14] However, care must be taken in the case of nanotube−graphene hybrid dispersions. It is well-known that sonication of graphene in liquids gives flakes with a wide range of lateral sizes. The size distribution in the final dispersion can be controlled by centrifugation (CF), with higher CF rates resulting in smaller flakes.[28,29] For films of graphene flakes alone, it is expected that large flakes should result in better electrical properties, as this should reduce the number of interflake junctions. However, this may not be so simple for graphene−nanotube hybrids as there may be an optimum flake size, commensurate with the typical pore size of the nanotube network. To test this, we decided to do an initial survey on the effect of varying graphene flake size on the opto-electrical properties of graphene−nanotube hybrid films.

The graphene suspensions were centrifuged at three different rotation rates, 1500, 5000, and 15 000 rpm for 90 min, while the nanotubes were centrifuged at 5500 rpm for 90 min. After centrifugation, the concentration of each dispersion was measured by optical absorption spectroscopy. To test the effect of rotation rate on graphene flake size, thin graphene films were prepared by vacuum filtration of the three centrifuged graphene dispersions. Raman spectroscopy (Horiba Jobin Yvon LAbRAM-HR, 633 nm) was carried out on these films. Five spectra were measured for each film. These were normalized and averaged to give the spectra shown in Figure 1A (the spectrum for the graphite

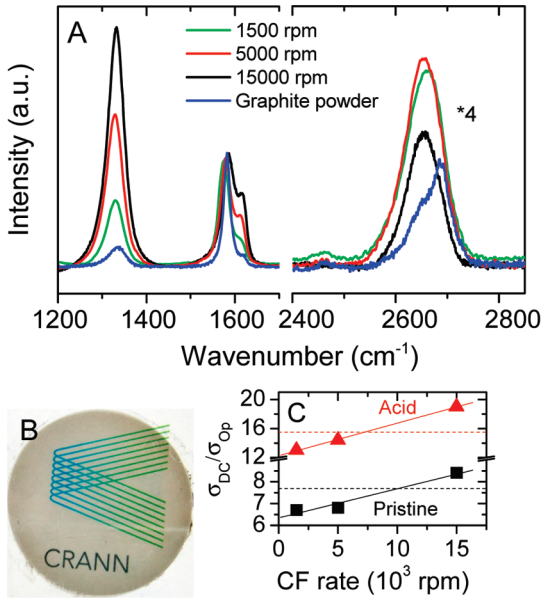

Figure 1. (A) Raman spectra of graphene films prepared from dispersions which had been centrifuged at different rates, 1500, 5000, and 15 000 rpm. The thin films were prepared by vacuum filtration of the graphene dispersions. Shown for comparison is a Raman spectrum of the starting graphite powder. N.B. The portion of the graph above 2400 cm^{-1} has been multiplied by a factor of 4 for clarity. (B) Photograph of a 60 nm thick, 3 wt % hybrid film after transfer onto PET. (C) Measured DC to optical conductivity ratio for hybrid films (3 wt % graphene) as a function of the centrifugation rate used during dispersion. Data are included for both pristine and acid-treated films. The horizontal dashed lines show the values of the conductivity ratio for nanotube-only films, both pristine and acid-treated.

powder is shown for comparison). The main difference between these spectra is the strong increase in D band (~1300 cm^{-1}) intensity with increasing centrifugation rate. It is known that the intensity of the D band relative to the G band (~1600 cm^{-1}) scales inversely with flake size.[28,29] This confirms that smaller flakes are retained for higher centrifugation rates. From the previously published relationship between the D/G intensity ratio and flake size,[29] we can estimate the average flake lengths to be ~400, ~650, and ~1300 nm for rotation rates of 15 000, 5000, and 1500 rpm, respectively (assuming a mean flake aspect ratio of 2.3).

The nanotube and graphene (three different rotation rates) dispersions were blended in the ratio required to give three hybrid dispersions, all with 3 wt % graphene (for justification of this composition, see below), but with different graphene flake sizes. Thin films were fabricated by vacuum filtration[12,14] at a fixed nominal thickness of 60 nm. This thickness was chosen to avoid the problem of thickness-dependent DC conductivity, which is often encountered in thin nanostructured films. For example, thin nanotube films only demonstrate thickness-independent DC conductivity at thicknesses above 40 nm.[14] Similarly, for graphene films, the DC conductivity only remains constant above thicknesses of 20 nm.[12] Below these thicknesses, the conductivity falls off due to network non-uniformity and percolative effects. A photograph of a 60 nm thick film (3 wt % graphene) is shown in Figure 1B.

We measured the transmittance and sheet resistance of the three, 3 wt % hybrids, each with different graphene flake size. In order to compare these hybrids as transparent conductors, we used T and R_s to calculate σ_{DC}/σ_{Op} using eq 1. We have plotted σ_{DC}/σ_{Op} as a function of CF rate used in the dispersion preparation in Figure 1C. These data clearly show that the film performance improves for higher rotation rates and so smaller graphene flakes. It is well-known that exposure to acid can remove residual surfactant and improve the quality of thin films of nanotubes (see below).[18] As such, we soaked the films in nitric acid for 2 h before measuring R_s and T and calculating σ_{DC}/σ_{Op} again. These data are also shown in Figure 1C and confirm that higher rotation rates give better films. In the future, it would be interesting to prepare dispersions at even higher CF rates to look for a downturn in the data. We note that, for both pristine and acid-treated films, no improvement over nanotube-only films (see dashed lines in Figure 1C) is seen for graphene dispersions centrifuged at rates below 7000−10 000 rpm. This shows that a maximum flake size exists, above which addition of graphene actually does not improve the films.

Film Morphology. With these results in mind, we prepared a series of hybrid films from graphene dispersions prepared at a CF rate of 15 000 rpm. These films were of a constant thickness of 60 nm but had graphene content varying from 0% (SWNT only) to 100%. Shown in Figure 2 is a set of representative SEM images of the surfaces of hybrids of various compositions after transfer to PET (t = 60 nm). Figure 2A is typical of a thin nanotube film, showing a random array of bundles and significant porosity. Figure 2B shows a 3 wt % graphene hybrid. Here a small number of isolated submicrometer graphene flakes appear dispersed within the nanotube matrix. As the graphene content is increased from Figure 2C to Figure 2E, the graphene flakes first appear to fill the pores between nanotubes before starting to dominate the films. Figure 2F is an image of graphene-only film which clearly shows the flake size to range from <100 nm to a few hundred nanometers.

The SEM images discussed above give no real information about the aggregation state of the graphene. However, we can get some information on the flake thickness from Raman spectroscopy. We measured the Raman spectra of the films described above. For each film, we measured five spectra, normalized, and averaged them to give a representative spectrum for each composition. A subset of these averaged spectra are shown in Figure 3A along with the spectrum of graphite powder for comparison. In general, as all hybrid spectra are dominated by the nanotube component, we focus on hybrids with low nanotube content. For

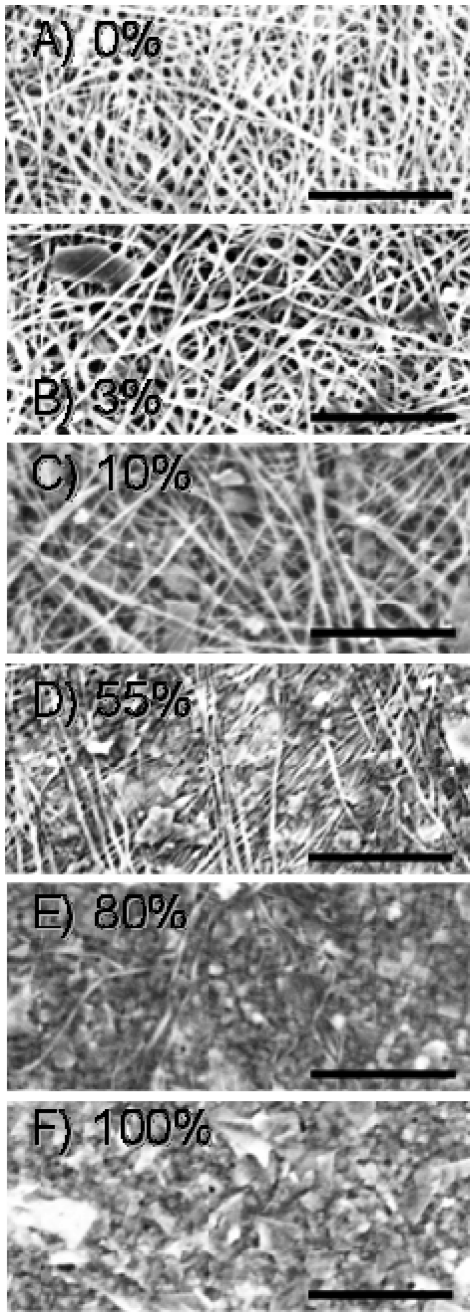

Figure 2. SEM images of some of the films studied in this work. (A) A 0% graphene (nanotube-only) film. Hybrid films with (B) 3, (C) 10, (D) 55, and (E) 80 wt % graphene. (F) A 100% graphene film. In all cases, the scale bar is 500 nm.

example, the G band (~1600 cm^{-1}) becomes dominated by the nanotube component even for the 90 wt % graphene film. However, of most interest is the 2D band close to 2600 cm^{-1}. The 2D band for the graphene-only film is clearly different than that of the graphite powder. For the graphene film, the more symmetric line shape is representative of graphene flakes with 2−5 layers[30,31] and shows that the flakes remain exfoliated, even during film formation. The 2D band of the 90 wt % graphene hybrid is dominated by the nanotube component. However, the shoulder due to the graphene component can be seen between 2650 and

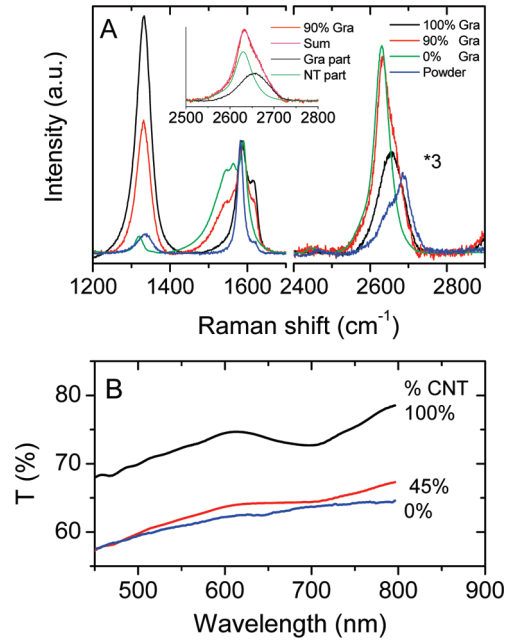

Figure 3. (A) Raman spectra for some of the films studied in this work, 100% graphene, 90% graphene, and 0% graphene (nanotube-only). Shown for comparison is a Raman spectrum of the starting graphite powder. N.B. The portion of the graph above 2400 cm^{-1} has been multiplied by a factor of 3 for clarity. Inset: Spectra for graphene-only (black) and nanotube-only (green) films. These spectra are just the spectra from the main image multiplied by 0.75 and 0.65, respectively. The sum of these weighted components (purple) gives a spectrum almost identical to the 90% graphene spectrum (red). (B) Transmittance spectra for a number of 60 nm thick films.

2700 cm^{-1}. This shoulder is at the same position as the graphene 2D band but is clearly too low in wavenumber to be associated with the graphite 2D band. This suggests that the graphene in the 90% film remains exfoliated even after film formation. If this is the case, the 2D band for the 90% graphene hybrid should be identical to a weighted summation of the 2D peaks for the nanotube-only and graphene-only films. This is illustrated in the inset where the peak marked "sum" is the weighted sum of the graphene and nanotube parts (also shown, these components were produced by weighting the curves in the main figure by factors of 0.75 and 0.65, respectively). The sum peak is almost identical to the measured peak for the 90% hybrid. This shows that, during film formation, graphene does not restack to form graphite but remains in the form of flakes with 2−5 layers. Given that this is the case for films with 90 and 100% graphene, it is very likely to hold for hybrids with lower graphene content.

Dependence of Optical and Electrical Properties on Film Composition. Optical transmission spectra were recorded for the films described above using a Varian Cary 6000i. All spectra were reasonably flat in the visible regime (Figure 3B). The transmittance ($\lambda = 550$ nm) is plotted as a function of mass fraction in Figure 4A (black squares). The transmittance decreases with increasing graphene content, falling from 73−70% for <10 wt %

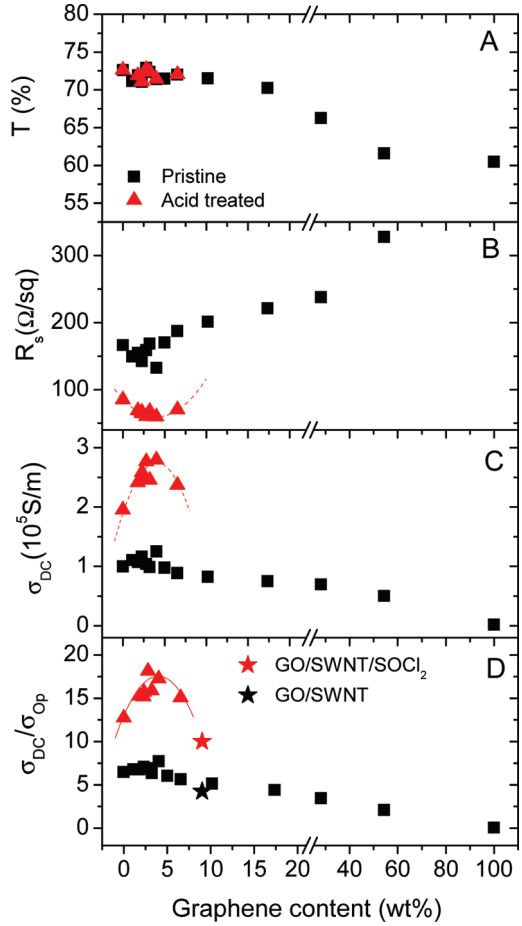

Figure 4. Optical and electrical properties of graphene/nanotube hybrid films as a function of graphene content for both pristine and acid-treated films. (A) Transmittance (550 nm), (B) sheet resistance, (C) DC conductivity, and (D) DC to optical conductivity ratio. In (B−D), the dashed line is a guide to the eye. Also marked in (D) are the results of Tung *et al.* for hydrazine-reduced graphene oxide/SWNT films both before and after doping with $SOCl_2$.

graphene samples to ~60% for the 100 wt % film. This is due to the fact that graphene is a highly absorbing material (each graphene sheet absorbs 2.3% of incident light[22]). While the optical conductivity for nanotube networks is close to $\sigma_{Op} = 1.7 \times 10^4$ S/m,[14] that for networks of graphene flakes is significantly higher, taking values up to $\sigma_{Op} = 2 \times 10^5$ S/m,[5,12] due to the higher optical conductivity of graphene itself.[22]

Sheet resistance (R_s) measurements were made using the four-probe technique with silver electrodes of dimensions and spacings typically of approximately millimeter size and a Keithley 2400 source meter. Shown in Figure 4B is the sheet resistance measured for ~60 nm thick hybrid films of varying graphene content. The sheet resistance of the 100% nanotube sample was 165 Ω/□. Interestingly, the resistance decreases slightly to a minimum of 140 Ω/□ for the 3 wt % graphene sample, before increasing steadily with increasing graphene content, reaching 8.4 kΩ/□ for the graphene-only film.

We can calculate the nominal direct current (DC) conductivity, σ_{DC}, from the sheet resistance using $\sigma_{DC} = (R_s t)^{-1}$, where t is the film thickness (Figure 4C). The DC conductivity increases from 10^5 S/m for the nanotube-only sample to a maximum of 1.2×10^5 S/m for the 3 wt % graphene sample before falling off to 2000 S/m for the graphene-only sample. The presence of a peak in DC conductivity is interesting as it suggests that addition of graphene can actually improve the electrical properties of nanotube-based films. This is in spite of the fact that graphene networks[5] tend to have DC conductivity significantly below 10^5 S/m (and lower than the best nanotube films[14,18,19]). However, it must be noted that it is very difficult to accurately measure the film thickness for nanostructured networks. This means that, while sheet resistance measurements are reliable, DC conductivity measurements can have significant error. Thus, the peak referred to above may not actually exist. This means that such an observation must be confirmed by a measurement which does not rely on accurate knowledge of film thickness.

In order to avoid the effects of inaccurate thickness measurements and to facilitate comparison with other systems, we can characterize the films in terms of the DC to optical conductivity ratio, σ_{DC}/σ_{Op}. Shown in Figure 4D are the calculated values of σ_{DC}/σ_{Op} as a function of graphene content. The conductivity ratio does indeed show a peak, increasing from 6.5 for the nanotube-only film to 7.6 for the 4 wt % graphene film before falling off to 0.08 for the graphene-only film. This peak is important as it illustrates the presence of an optimum composition. Higher values of σ_{DC}/σ_{Op} result in better transparent conductors. Thus, addition of very small amounts of graphene can noticeably improve the properties of the material. This is vital for materials such as nanotubes where only marginal improvements in performance have been observed in recent years.

We note that the values of σ_{DC} and σ_{DC}/σ_{Op} for the nanotube-only films are slightly lower than expected for these tubes.[14,18] These results were obtained from a recently purchased batch of arc discharge SWNTs (ILIIN Nanotech.), which gave films of slightly lower conductivity than previous batches (possibly due to shorter tube length distribution[32]). However, we note that similar improvements at low graphene content were also observed for preliminary measurements made with a previous, more conductive batch of nanotubes.[14] With that batch, we obtained NT films and hybrids with conductivity ratios of 10.5 and 13.5, respectively (no acid treatment). We note that $\sigma_{DC}/\sigma_{Op} \sim 10$ is close to the best reported performance of nanotube films without post-treatment.[13,14,18,23] (Acid treatment generally results in the increase in performance to $\sigma_{DC}/\sigma_{Op} = 25-35$.)[18,23] This shows that the observed improvements apply to near-superlative films rather than just films with lower performance.

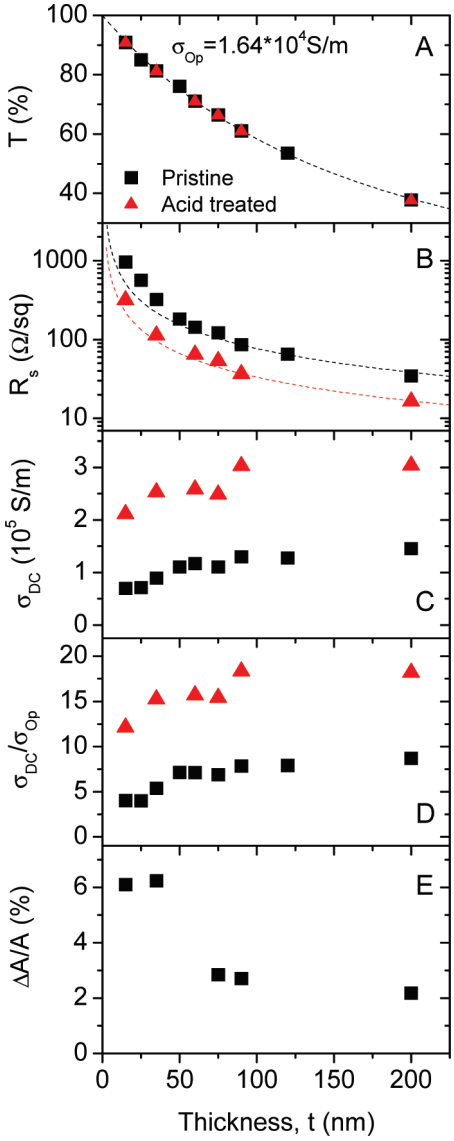

Figure 5. Optical and electrical properties of graphene/nanotube hybrid films with optimized graphene content (3 wt %), as a function of film thickness both before and after acid treatment. (A) Transmittance (550 nm), (B) sheet resistance, (C) DC conductivity, (D) DC to optical conductivity ratio, and (E) optical non-uniformity of films. In (A), the dashed line is fit to eq 2. In (B), the dashed lines represent bulk behavior as described by $R_s = (\sigma_{DC}t)^{-1}$ with $\sigma_{DC} = 1.3 \times 10^5$ and 3×10^5 S/m for the pristine and acid-treated films, respectively. Note the deviation from bulk behavior for $t < 50$ nm. This is also seen in (D) and (E).

We can compare the data in Figure 4D with the results of Tung *et al.* on hydrazine-reduced graphene oxide/nanotube films.[24] Their best results were for a graphene oxide content of ~8%, where we calculate that they achieved $\sigma_{DC}/\sigma_{Op} = 4$. Interestingly, this datum falls close to our data (Figure 4D).

Film Thickness Dependence. From our data, we identified an optimum composition of 3 wt % graphene and prepared films with a range of nominal thicknesses from $t = 15$ to 200 nm. As t increases, T falls off monotonically, as shown in Figure 5A. We can model this behavior using the expression[10]

$$T = (1 + Z_0\sigma_{Op}t/2)^{-2} \quad (2)$$

The fit is excellent, giving $\sigma_{Op} = 1.64 \times 10^4$ S/m, similar to the values of $1.5-2.0 \times 10^4$ S/m reported for nanotube films.[14,33,34]

In addition, R_s decreases with increasing thickness, reaching ~40 Ω/□ for $t = 200$ nm. We note that anomalously high R_s was observed at lower film thicknesses. This can be seen in the slight deviation between the measured data in Figure 5B and the dashed line that illustrates bulk-like behavior (defined by $\sigma_{DC} = 1.3 \times 10^5$ S/m). This can be seen more clearly by plotting σ_{DC} or σ_{DC}/σ_{Op} (Figure 5C,D) *versus* thickness. Both quantities are reasonably constant for $t > 40$ nm, displaying values of $\sigma_{DC} = 1.5 \times 10^5$ S/m and $\sigma_{DC}/\sigma_{Op} = 8$. However, for thinner films, both fall off significantly. This is commonly observed in thin films of nanostructured materials and occurs when the film thickness approaches the dimensions of the nanostructure making up the film (*i.e.*, the nanotube bundle diameter or the graphene flake thickness).[11,12,14,18] This phenomenon has been attributed to a combination of percolative effects and thickness non-uniformity at low thickness. Similar trends have been observed for films of carbon nanotubes,[14,18] graphene,[12] and silver nanowires.[11] We can gauge the thickness non-uniformity by measuring the spatially resolved transmittance (pixel size 5 μm) using a transmission scanner,[14] defining the non-uniformity as the standard deviation of local absorbance divided by the mean absorbance, $\Delta A/A$. This parameter is plotted in Figure 5E. $\Delta A/A$ is constant for thicknesses above 40 nm. Below this, the non-uniformity increases substantially.

We plot transmittance *versus* sheet resistance for varying thickness (3 wt % graphene) in Figure 6. Equation 1 can be fitted to these data with a good fit obtained for films with $t > 40$ nm. This fit gives a value of $\sigma_{DC}/\sigma_{Op} \approx 8$ for the as-prepared films. Shown in the inset is an image of a thin ($t = 25$ nm) 3 wt % hybrid. The

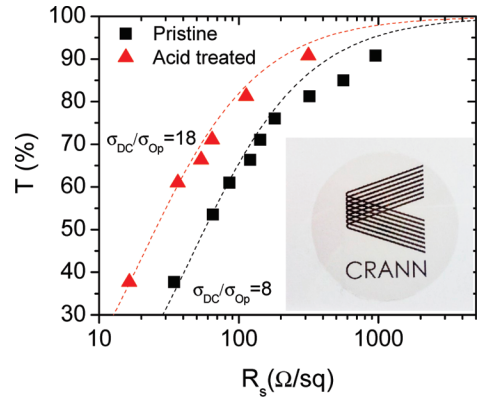

Figure 6. Opto-electrical properties of hybrid films with optimized graphene content (3 wt %). Transmittance (550 nm) is plotted as a function of sheet resistance for both as-produced films and acid-treated films. The dashed lines are fits to eq 1. Inset: Photograph of a thin ($t = 25$ nm, $T = 85\%$) 3 wt % hybrid.

transmittance of this film was 85%. It is clear from this image that the optical quality of this film is excellent.

Acid Treatment. It is well-known that acid treatment significantly reduces R_s for nanotube networks[18] due to reduction of junction resistance.[23] Such treatment typically results in reduction in resistance by a factor of 3.[18] Hence, we have treated a number of films of varying mass fraction around the optimum (3 wt %) by soaking them in concentrated nitric acid and rinsing with water.[23] We measured the transmittance and sheet resistance of such films. In addition, we calculated σ_{DC} and σ_{DC}/σ_{Op}. While it does not affect the film transmittance (Figure 4A), acid treatment reduces R_s by a factor of 2.5−3, as shown in Figure 4B. We observed a well-defined peak in the R_s *versus* composition curve with a minimum sheet resistance of $R_s = 60\ \Omega/\square$ at a graphene content of 3 wt %. In addition, commensurate increases were observed for both σ_{DC} and σ_{DC}/σ_{Op} (Figure 4C,D). Notably, the peaks in σ_{DC} and σ_{DC}/σ_{Op} become much more well-defined, confirming the presence of an optimum composition. The best results occur for the acid-treated 2.8 wt % graphene film which displays $\sigma_{DC} = 2.8 \times 10^5$ S/m and $\sigma_{DC}/\sigma_{Op} = 18$. Thus, after acid treatment, addition of graphene to a nanotube film results in an increase in σ_{DC}/σ_{Op} from 12.5 to 18, an increase of 40%. Tung *et al.* chemically treated their graphene oxide/nanotube films with $SOCl_2$, achieving $\sigma_{DC}/\sigma_{Op} = 10$. We note that our best results are significantly higher. This, coupled with the simplicity of our technique, makes this a promising process.

We have also measured the thickness dependence of the optical and electrical properties of the acid-treated films, as shown in Figure 5A−D. As with the pristine films, both σ_{DC} and σ_{DC}/σ_{Op} are constant at thickness >40 nm but tend to fall off at lower thickness. Shown in Figure 6 is the transmittance for the acid-treated films plotted as a function of sheet resistance. This shows that we can achieve films with transmittance of 80% coupled with a sheet resistance of 100 $\Omega/\square$. We note that these acid-treated films are very stable. We have measured the transmittance and sheet resistance of the films shown in Figure 6 three months after preparation. No discernible changes in the properties were found. Similar stability was found by Dan *et al.* for acid-treated nanotube films.[9]

Mechanism. It is important to understand the nature of the peak in DC conductivity, and hence σ_{DC}/σ_{Op}, for compositions close to 3 wt %. It is known that the conductivity of carbon nanotube networks is limited by the intertube junction resistance.[23,35] We propose that the junction resistance between a nanotube and a graphene flake may be significantly smaller than that between two nanotubes (or two bundles). Thus, the presence of a graphene sheet in contact with two nearby nanotubes could act to circumvent the nanotube−nanotube junction and promote internanotube charge transport. This would be manifested by an increase in the conductivity of the film. Within this hypothesis, addition of small amounts of graphene should result in a conductivity increase which scales with graphene content. However, as the graphene content is increased further, the graphene may act to swell the nanotube network, thus increasing the resistance of the nanotube−nanotube junctions still carrying appreciable current. This would be manifested by a turnover and subsequent drop in film conductivity. This scenario is supported by the data presented in Figure 1C, which shows the film performance improve as the graphene flake size decreases. It is likely that smaller flakes can fit into the space between SWNTs without deforming the network. As the graphene content is increased further, the electrical properties of the film become dominated by the graphene with the DC conductivity approaching that for a graphene-only film. This model is also consistent with the observation that the electrical properties improve markedly on acid treatment. Exposure to acid tends to remove residual surfactant, resulting in a decrease in junction resistance.[23,33] Surfactant removal may be more effective for nanotube−graphene junctions resulting in an amplification of the peak after acid treatment.

This model suggests that the graphene flake size is critical to the performance of these networks. Further work would involve accurate measurement of the optimum flake size. In addition, it will be critical to measure the nanotube−graphene junction resistance to compare it to the nanotube−nanotube junction resistance.

CONCLUSIONS

In conclusion, we have demonstrated a simple, water-based technique to prepare graphene−nanotube hybrid films. By adding small quantities of graphene to nanotube networks, the DC conductivity can be enhanced without reducing the optical transmittance. The graphene flake size is critical to this process, with smaller flakes giving better results. The results are further improved by acid treatment of the films. Addition of 3 wt % graphene results in an increase of the materials figure of merit by 40%. We believe that the strength of this process is that it can be used to improve already good quality films.

METHODS

We prepared graphene dispersions by adding graphite (Branwell natural graphite, grade 2369) to a solution of sodium cholate (NaC) surfactant in water (0.1 mg/mL NaC) such that the graphite concentration was 5 mg/mL. This dispersion was then sonicated in a sonic bath (power output 14.7 W) for 48 h. The resulting dispersion was left to stand for 24 h to allow any unstable aggregates to form. This was then centrifuged at 1500, 5000, or 15 000 rpm for 90

min (Hettich Mikro 22R). After centrifugation, the top 80% of supernatant was decanted and retained for use.

We prepared nanotube (Iljin nanotech) dispersions in a similar manner by adding nanotubes to a solution of NaC surfactant in water (5 mg/mL NaC) such that the nanotube concentration was 1 mg/mL. This dispersion was subjected to 5 min of high-power tip sonication (VibraCell CVX; 750 W, 20% 60 kHz), then placed in a sonic bath for 1 h, and then subjected to another 5 min of high-power sonication. They were then allowed to rest overnight before being centrifuged at 5500 rpm for 90 min. The supernatant was carefully decanted and saved.

We measured the concentration after centrifugation by measuring the absorbance spectrum of each dispersion and recording the absorbance per unit cell length, A/l, at 660 nm. From the Lambert−Beer law, this gives the concentration once the extinction coefficient, α, is known ($A = \alpha Cl$). The extinction coefficient for surfactant-dispersed nanotubes has been measured to be $\alpha_{SWNT} = 3389$ mL mg^{-1} m^{-1}.[36] We determined the extinction coefficient for the NaC-dispersed graphene by measuring A/l at 660 nm for a large known volume of dispersion, sonication time 24 h, centrifugation rate 5000 rpm. This dispersion (in excess of 400 mL volumes) was filtered through a preweighed porous membrane. The membrane was dried and reweighed to give the deposited mass. The proportion of graphitic mass on the filter membrane was determined using TGA analysis. This gave a value of $\alpha_G = 6600$ mL mg^{-1} m^{-1}.

Once the concentrations were determined, these dispersions were blended in the ratio required to give the desired graphene/nanotube mass fraction. Mass fractions between 0 and 100% graphene were prepared. The mixtures were then sonicated for 15 min in a sonic bath to homogenize.

The resulting dispersions were vacuum-filtered using porous cellulose filter membranes (MF-Millipore membrane, mixed cellulose esters, hydrophilic, 0.025 μm, 47 mm) to give thin films. The thickness of these films was controlled by the volume of dispersion filtered and hence the deposited mass.

The deposited films were washed with 200 mL of Millipore water followed by a wet transfer to a polyethylene terephthalate (PET) substrate using heat and pressure.[19] The cellulose filter membrane was then removed by treatment with acetone vapor and subsequent acetone liquid baths followed by a methanol bath. The final film diameter was 36 mm. For acid treatment, films were immersed in 65% nitric acid for for 2 h followed by rinsing with Millipore water.

Optical transmission spectra were recorded in the visible range (400−800 nm) using a Varian Cary 6000i. In all cases, PET was used as the reference. R_s measurements were made using the four-probe technique with silver electrodes of dimensions and spacings typically of approximately millimeter size and a Keithley 2400 source meter. Transmission scans were made using an Epson Perfection V700 photo flat-bed transmission scanner with a bit depth of 48 bits per pixel and a spatial resolution of 6400 dpi. SEM measurements were made using a Zeiss Ultra plus SEM. Raman spectra were obtained using (Horiba Jobin Yvon LAbRAM-HR, 633 nm) on films transferred to glass substrates.

Acknowledgment. This work was funded by SFI PI Grant 07/IN.1/I1772 as well as the SFI funded CRANN-HP collaboration 08/CE/I1432s1.

REFERENCES AND NOTES

1. Gordon, R. G. Criteria for Choosing Transparent Conductors. *MRS Bull.* **2000**, *25*, 52.
2. Chen, Z.; Cotterell, B.; Wang, W. The Fracture of Brittle Thin Films on Compliant Substrates in Flexible Displays. *Eng. Fract. Mech.* **2002**, *69*, 597–603.
3. Leterrier, Y.; Medico, L.; Demarco, F.; Manson, J. A. E.; Betz, U.; Escola, M. F.; Olsson, M. K.; Atamny, F. Mechanical Integrity of Transparent Conductive Oxide Films for Flexible Polymer-Based Displays. *Thin Solid Films* **2004**, *460*, 156–166.
4. Pammi, S. V. N.; Chanda, A.; Seong, N. J.; Yoon, S. G. Growth of High-Quality ITO Thin Films at Low Temperature by Tuning the Oxygen Flow Rate Using the Nano-Cluster Deposition (NCD) Technique. *Chem. Phys. Lett.* **2010**, *490*, 234−237.
5. De, S.; Coleman, J. N. Are There Fundamental Limitations on the Sheet Resistance and Transmittance of Thin Graphene Films? *ACS Nano* **2010**, *4*, 2713−2720.
6. Ghosh, D. S.; Chen, T. L.; Pruneri, V. Ultrathin Cu−Ti Bilayer Transparent Conductors with Enhanced Figure-of-Merit and Stability. *Appl. Phys. Lett.* **2010**, *96*, 091106.
7. Ghosh, D. S.; Chen, T. L.; Pruneri, V. High Figure-of-Merit Ultrathin Metal Transparent Electrodes Incorporating a Conductive Grid. *Appl. Phys. Lett.* **2010**, *96*, 041109.
8. Hu, L.; Hecht, D. S.; Gruner, G. Percolation in Transparent and Conducting Carbon Nanotube Networks. *Nano Lett.* **2004**, *4*, 2513–2517.
9. Dan, B.; Irvin, G. C.; Pasquali, M. Continuous and Scalable Fabrication of Transparent Conducting Carbon Nanotube Films. *ACS Nano* **2009**, *3*, 835–843.
10. Dressel, M.; Gruner, G. *Electrodynamics of Solids: Optical Properties of Electrons in Matter*; Cambridge University Press: Cambridge, UK, 2002.
11. De, S.; Higgins, T. M.; Lyons, P. E.; Doherty, E. M.; Nirmalraj, P. N.; Blau, W. J.; Boland, J. J.; Coleman, J. N. Silver Nanowire Networks as Flexible, Transparent, Conducting Films: Extremely High DC to Optical Conductivity Ratios. *ACS Nano* **2009**, *3*, 1767–1774.
12. De, S.; King, P. J.; Lotya, M.; O'Neill, A.; Doherty, E. M.; Hernandez, Y.; Duesberg, G. S.; Coleman, J. N. Flexible, Transparent, Conducting Films of Randomly Stacked Graphene from Surfactant-Stabilized, Oxide-Free Graphene Dispersions. *Small* **2010**, *6*, 458–464.
13. De, S.; Lyons, P. E.; Sorrel, S.; Doherty, E. M.; King, P. J.; Blau, W. J.; Nirmalraj, P. N.; Boland, J. J.; Scardaci, V.; Joimel, J.; Coleman, J. N. Transparent, Flexible, and Highly Conductive Thin Films Based on Polymer−Nanotube Composites. *ACS Nano* **2009**, *3*, 714–720.
14. Doherty, E. M.; De, S.; Lyons, P. E.; Shmeliov, A.; Nirmalraj, P. N.; Scardaci, V.; Joimel, J.; Blau, W. J.; Boland, J. J.; Coleman, J. N. The Spatial Uniformity and Electromechanical Stability of Transparent, Conductive Films of Single Walled Nanotubes. *Carbon* **2009**, *47*, 2466–2473.
15. Lee, J. Y.; Connor, S. T.; Cui, Y.; Peumans, P. Solution-Processed Metal Nanowire Mesh Transparent Electrodes. *Nano Lett.* **2008**, *8*, 689–692.
16. Gaynor, W.; Lee, J. Y.; Peumans, P., Fully Solution-Processed Inverted Polymer Solar Cells with Laminated Nanowire Electrodes. *ACS Nano* **2010**, *4*, 30−34.
17. Lee, J. Y.; Connor, S. T.; Cui, Y.; Peumans, P. Semitransparent Organic Photovoltaic Cells with Laminated Top Electrode. *Nano Lett.* **2010**, *10*, 1276−1279.
18. Geng, H. Z.; Kim, K. K.; So, K. P.; Lee, Y. S.; Chang, Y.; Lee, Y. H. Effect of Acid Treatment on Carbon Nanotube-Based Flexible Transparent Conducting Films. *J. Am. Chem. Soc.* **2007**, *129*, 7758–7759.
19. Wu, Z. C.; Chen, Z. H.; Du, X.; Logan, J. M.; Sippel, J.; Nikolou, M.; Kamaras, K.; Reynolds, J. R.; Tanner, D. B.; Hebard, A. F.; Rinzler, A. G. Transparent, Conductive Carbon Nanotube Films. *Science* **2004**, *305*, 1273–1276.
20. Becerril, H. A.; Mao, J.; Liu, Z.; Stoltenberg, R. M.; Bao, Z.; Chen, Y. Evaluation of Solution-Processed Reduced Graphene Oxide Films as Transparent Conductors. *ACS Nano* **2008**, *2*, 463–470.
21. Wang, X.; Zhi, L.; Mullen, K. Transparent, Conductive Graphene Electrodes for Dye-Sensitized Solar Cells. *Nano Lett.* **2007**, *8*, 323–327.
22. Nair, R. R.; Blake, P.; Grigorenko, A. N.; Novoselov, K. S.; Booth, T. J.; Stauber, T.; Peres, N. M. R.; Geim, A. K. Fine Structure Constant Defines Visual Transparency of Graphene. *Science* **2008**, *320*, 1308.
23. Nirmalraj, P. N.; Lyons, P. E.; De, S.; Coleman, J. N.; Boland, J. J. Electrical Connectivity in Single-Walled Carbon Nanotube Networks. *Nano Lett.* **2009**, *9*, 3890–3895.
24. Tung, V. C.; Chen, L. M.; Allen, M. J.; Wassei, J. K.; Nelson, K.; Kaner, R. B.; Yang, Y. Low-Temperature Solution Processing of Graphene−Carbon Nanotube Hybrid

Materials for High-Performance Transparent Conductors. *Nano Lett.* **2009**, *9*, 1949–1955.
25. Hernandez, Y.; Lotya, M.; Rickard, D.; Bergin, S. D.; Coleman, J. N. Measurement of Multicomponent Solubility Parameters for Graphene Facilitates Solvent Discovery. *Langmuir* **2010**, *26*, 3208–3213.
26. Hernandez, Y.; Nicolosi, V.; Lotya, M.; Blighe, F. M.; Sun, Z. Y.; De, S.; McGovern, I. T.; Holland, B.; Byrne, M.; Gun'ko, Y. K.; Boland, J. J.; Niraj, P.; Duesberg, G.; Krishnamurthy, S.; Goodhue, R.; Hutchison, J.; Scardaci, V.; Ferrari, A. C.; Coleman, J. N. High-Yield Production of Graphene by Liquid-Phase Exfoliation of Graphite. *Nat. Nanotechnol.* **2008**, *3*, 563–568.
27. Lotya, M.; Hernandez, Y.; King, P. J.; Smith, R. J.; Nicolosi, V.; Karlsson, L. S.; Blighe, F. M.; De, S.; Wang, Z.; McGovern, I. T.; Duesberg, G. S.; Coleman, J. N. Liquid Phase Production of Graphene by Exfoliation of Graphite in Surfactant/Water Solutions. *J. Am. Chem. Soc.* **2009**, *131*, 3611–3620.
28. Khan, U.; O'Neill, A.; Lotya, M.; De, S.; Coleman, J. N. High-Concentration Solvent Exfoliation of Graphene. *Small* **2010**, *6*, 864–871.
29. Lotya, M.; King, P. J.; Khan, U.; De, S.; Coleman, J. N. High-Concentration, Surfactant-Stabilized Graphene Dispersions. *ACS Nano* **2010**, *4*, 3155−3162.
30. Ferrari, A. C.; Meyer, J. C.; Scardaci, V.; Casiraghi, C.; Lazzeri, M.; Mauri, F.; Piscanec, S.; Jiang, D.; Novoselov, K. S.; Roth, S.; Geim, A. K. Raman Spectrum of Graphene and Graphene Layers. *Phys. Rev. Lett.* **2006**, *97*, 187401.
31. Malard, L. M.; Pimenta, M. A.; Dresselhaus, G.; Dresselhaus, M. S. Raman Spectroscopy in Graphene. *Phys. Rep.* **2009**, *473*, 51–87.
32. Hecht, D.; Hu, L. B.; Gruner, G. Conductivity Scaling with Bundle Length and Diameter in Single Walled Carbon Nanotube Networks. *Appl. Phys. Lett.* **2006**, *89*, 133112.
33. Geng, H. Z.; Lee, D. S.; Kim, K. K.; Han, G. H.; Park, H. K.; Lee, Y. H. Absorption Spectroscopy of Surfactant-Dispersed Carbon Nanotube Film: Modulation of Electronic Structures. *Chem. Phys. Lett.* **2008**, *455*, 275–278.
34. Ruzicka, B.; Degiorgi, L.; Gaal, R.; Thien-Nga, L.; Bacsa, R.; Salvetat, J. P.; Forro, L. Optical and Dc Conductivity Study of Potassium-Doped Single-Walled Carbon Nanotube Films. *Phys. Rev. B* **2000**, *61*, R2468–R2471.
35. Topinka, M. A.; Rowell, M. W.; Goldhaber-Gordon, D.; McGehee, M. D.; Hecht, D. S.; Gruner, G. Charge Transport in Interpenetrating Networks of Semiconducting and Metallic Carbon Nanotubes. *Nano Lett.* **2009**, *9*, 1866–1871.
36. Bergin, S. D.; Nicolosi, V.; Cathcart, H.; Lotya, M.; Rickard, D.; Sun, Z. Y.; Blau, W. J.; Coleman, J. N. Large Populations of Individual Nanotubes in Surfactant-Based Dispersions without the Need for Ultracentrifugation. *J. Phys. Chem. C* **2008**, *112*, 972–977.